Studies Into the Use of Non-linear Ultrasound to Detect Corroded Steel Plates Embedded in Concrete

Nilsson, Markus; Ulriksen, Peter; Rydén, Nils

Published in:
Proceedings of the International Conference on Non-destructive Evaluation of Concrete in Nuclear Applications

2023

Document Version:
Publisher's PDF, also known as Version of record

Studies Into the Use of Non-linear Ultrasound to Detect Corroded Steel Plates Embedded in Concrete

Markus Nilsson[1,*], Peter Ulriksen[1] and Nils Rydén[1]
[1] Lund University, Faculty of Engineering, Division of Engineering Geology, Lund, Sweden

ABSTRACT

In some nuclear power plants, the containment liners are embedded in concrete. The purpose of the containment liner is to minimize the risk of radioactive leakage by granting a leak-tight containment building. In the presence of flaws in the surrounding concrete, such as voids, or foreign objects embedded in the concrete, there is a risk that the liner plate might corrode. This could degrade the leak tightness of the containment building, leading to an increased risk of radioactive leakage. A project is being carried out at Lund University whose purpose is to assess the capability of non-linear ultrasound to detect corroded steel plates embedded in concrete. Second harmonic analysis has been used to determine if general corrosion induced an increase in acoustical non-linearity. This was done by inspecting a steel plate with varying grades of corrosion immersed in water. Results from this study indicated that severe corrosion increases the relative parameter of quadratic non-linearity (β'). β' is given by the ratio between the second harmonic amplitude and the fundamental amplitude squared. Building on this result, initial findings from modulation experiments on concrete cylinders with embedded steel plates with varying grades of corrosion are presented.

Keywords: Corrosion; containment liner; non-linear ultrasound

1. INTRODUCTION

The containment liner plates (CLP) in some Nuclear Power Plants (NPPs) are to a certain extent embedded in concrete. The purpose of the CLP is to ensure leak-tightness so that no radioactive particles are leaked into the surrounding environment. Due to the alkaline environment inside the concrete, steel should not corrode at an alarming rate. However, in the presence of flaws in the concrete or embedded foreign objects, the passivity might be compromised. This would cause the steel to corrode aggressively which will damage the leak tightness. It is therefore important to be able to detect corrosion in embedded CLP.

A project is being carried out at Lund University whose aim is to assess the feasibility of using non-linear ultrasonics to detect corroded CLP embedded in concrete. Conventional (linear) ultrasound uses parameters that are mainly linear, such as the time-of-flight, attenuation, and sound velocity. The resolution of these methods is restricted by the frequency of the ultrasound, meaning that the wavelength of the probing wave must be less than or equal to the defect size. As concrete is a highly attenuative material due to its heterogeneous nature, high-frequency (MHz-range) ultrasound is unsuitable for this application. However, research has shown that ultrasound with wavelengths some order of magnitude greater than the defect size may distort due to locally enhanced elastic nonlinearity at the defects [1], [2]. This distortion generates new spectral components in the propagated sound wave. In monochromatic ultrasound, the distortion causes the generation of higher harmonics, i.e., integer multiples of the fundamental frequency [3]. In the case of polychromatic excitations, in addition to higher-harmonics, modulation frequencies, i.e., sidebands, around the excitation frequencies are generated [4]. In non-linear ultrasound, parameters based on these spectral components are studied and used as damage indices. This work

* Corresponding author: Markus.nilsson@tg.lth.se

presents results from two investigations. The first investigation, which has been published in [5], studies second harmonic generation in a uniformly corroded steel plate. Building on those results, the second case investigates the inspection of concrete cylinders containing embedded plates using non-classical non-linearities and some initial results are presented here.

Considering that steel plates are conventionally manufactured by rolling, a metalworking process that pushes material through a series of rolls to reduce the thickness of the material, it is assumed that this process creates surface-plane parallel internal structures in the bulk material. When the plate then corrodes, the affected volume delaminates and cracks. Examples of this can be viewed in Figure 1, where X-ray tomography shows the cross-section of two corrosion products of different origins. The sheet-type corrosion product in Figure 1 a) was found on a uniformly corroded steel plate found at a scrap yard. Its thickness is roughly 2 mm. The 15 mm thick corrosion product in Figure 1 b) was extracted from the CLP in the containment building housing the nuclear reactor Ringhals 3 in Sweden. Both corrosion products exhibit similar delamination characteristics and have several cracks and voids.

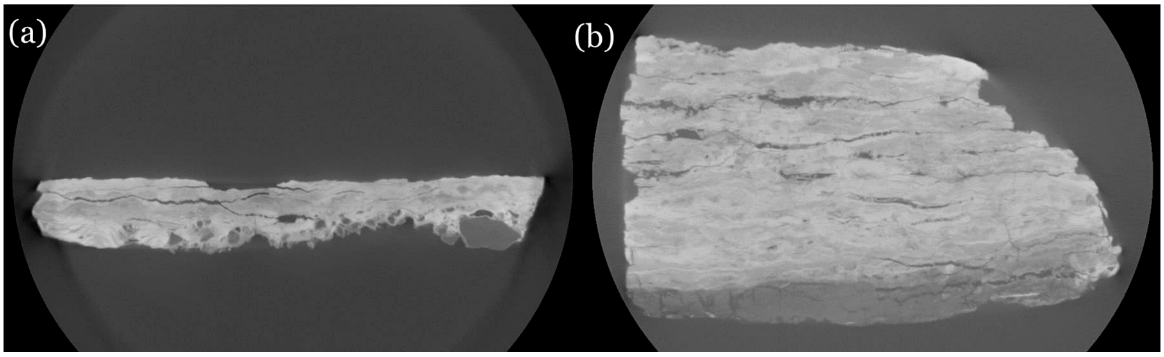

Figure 1. X-ray tomography showing; (a) the cross-section of a piece of sheet-type corrosion studied in the present work; (b) the cross-section of a corrosion product obtained from the Ringhals 3 containment wall. Reproduced from [5].

2. MEASURED PARAMETERS IN NON-LINEAR ULTRASOUND

2.1 Relative Parameter of Quadratic Non-linearity

By formulating Newton's second law of motion in terms of particle displacements (u), a non-linear wave equation can be obtained given that the stress term is expanded in a power series including first-order non-linearity. The solution will only include the fundamental component (u_1) and the second harmonic (u_2), given that the boundary condition at the source is a monochromatic excitation. This enables us to formulate an expression for the parameter of quadratic non-linearity (β) in terms of particle displacements (u):

$$\beta = \frac{8u_2}{u_1^2 k^2 x} \tag{2}$$

Where k is the wave number, and x is the propagation distance. It may be impractical to measure the particle displacement in engineering NDT applications. Fortunately, the received voltage signals from an ultrasonic transducer are proportional to the displacements, and they may be used to obtain relative measures of β. This relative parameter, given by Eq. (3), is denoted β', and is thus given by the second harmonic (A_2) and the fundamental amplitude squared (A_1^2) of the received voltage signal. Taking several measurements with increasing excitation amplitude enables the determination of averaged β'-values.

$$\beta \propto \beta' = \frac{A_2}{A_1^2} \tag{3}$$

2.2 Sideband Energy Distribution

The theory of classical power-series type non-linearity cannot adequately describe certain observed phenomena. Cross-modulation between a probe-wave and a strong amplitude-modulated (AM) wave (analogous to the Luxembourg-Gorky (LG) effect [6] in radio waves) is one such phenomenon [7], [8]. By integrating the power spectrum in appropriate intervals, the energy in the sidebands (E_{sb}) and probe-component (E_p) can be determined. This can be used to determine a parameter of non-linearity α, see Eq. (4).

$$\alpha = \frac{E_{sb}}{E_p} \tag{4}$$

3. EXPERIMENTS

3.1 Second Harmonic Analysis

3.1.1 Uniformly Corroded Steel Plate

The steel plate used to study the potential of non-linear ultrasound to detect corrosion is seen in Figure 2. The plate consisting of ordinary steel was initially uniformly corroded (*COR*) and covered by a thin sheet of corrosion (*SCOR*), here called sheet corrosion (see Figure 1 a) for a cross-sectional view of a sheet corrosion product). The sheet corrosion was separated from the steel plate during handling, and due to being very brittle, it broke into multiple pieces. One of the largest pieces was reattached to the plate by gluing it with ethyl-cyanoacrylate. As the plate was to be immersed in water, the sheet corrosion was painted in water-resistant varnish before being reattached to the plate. Half of the uniformly corroded plate was ground to remove the top corrosion layer. This was performed to achieve a region deemed flawless, thus "*OK*". Figure 2 shows the measurement point placement used in the indexed measurements. As shown, there are a total of 6 measurement points in the OK region, 4 in COR, and 2 in SCOR.

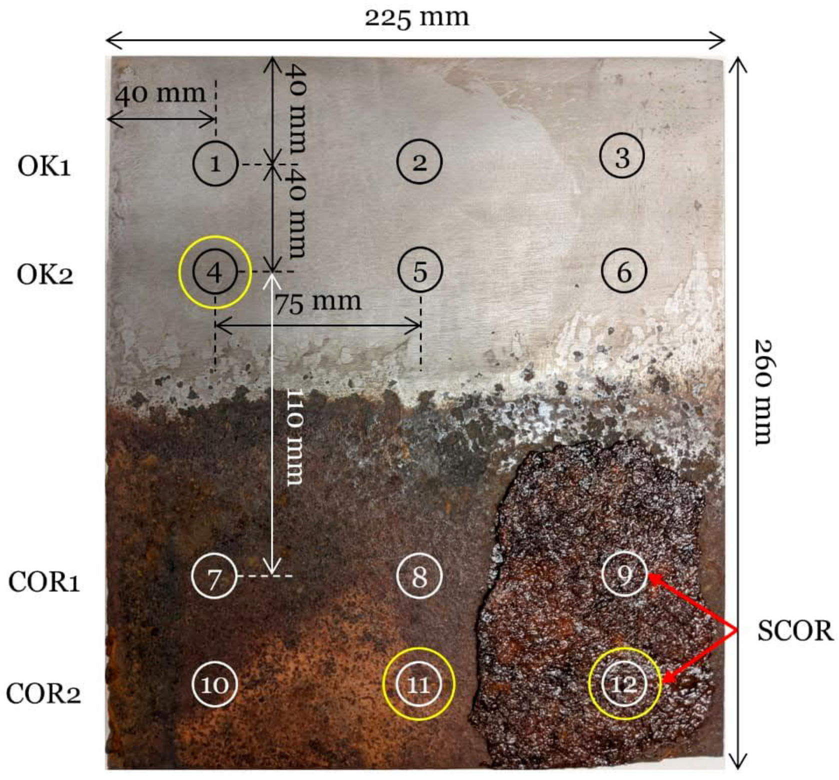

Figure 2. The corroded steel plate used in the presented work. Reproduced from [5].

3.1.2 Experimental Setup

The experimental setup for the second harmonic analysis used to inspect the steel plate (Figure 2) is illustrated schematically in Figure 3. A 4-cycle sine burst with a fundamental frequency of 4.5 MHz was used as the probe signal. The high frequency was used to avoid the generation of spurious harmonics. The signal was amplified in two steps before being sent to the transmitter (T in Figure 3). The voltage levels used were 14, 30, 47, 63, 74, and 80 V_{pp} measured at the 50 Ω load before the transducer. The transducer used was an immersion-type transducer from Olympus (V309-SU) with a center frequency of 4.5 MHz. The receiving hydrophone (SEA SPRH-S-1000, R in Figure 3) has good sensitivity in the range of 1.5 MHz - 10 MHz. The received signal was amplified before being collected in the oscilloscope. The collected data was post-processed (windowing, DFT, and more) on a PC with the MATLAB environment. A manual XY-scanner was used to move the transmitter-receiver pair equally and consistently across the plate.

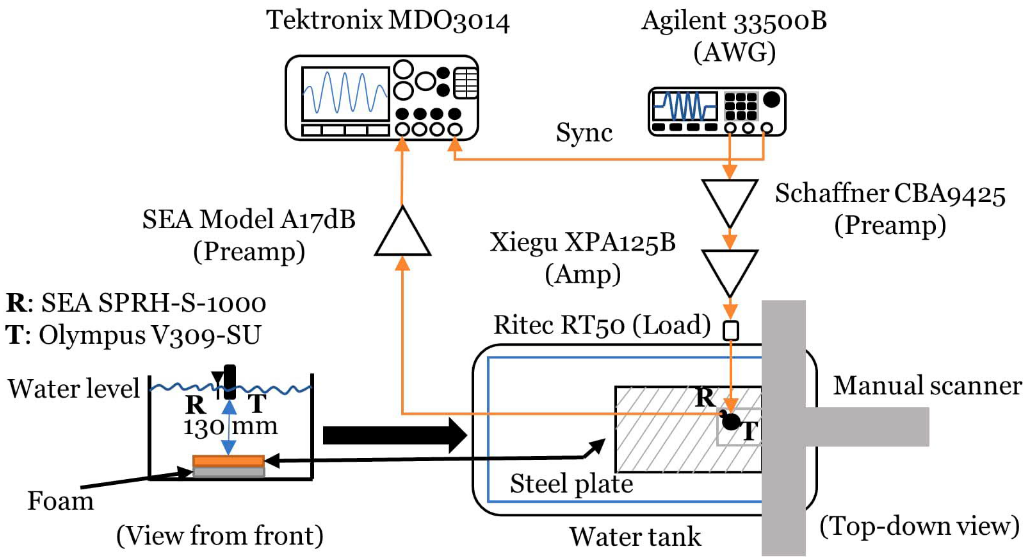

Figure 3. Experimental setup used for the measurements carried out for the second-harmonic analysis. Reproduced from [5].

3.2 Cross-Modulation Experiment

3.2.1 Concrete Cylinders with Embedded Steel Plates

A total of five concrete cylinders were prepared for the modulation experiments. One cylinder did not contain any steel plate discs, but the remaining cylinders did. The plate discs that were embedded in concrete can be seen in Figure 4. Plate COR is uniformly corroded and so was SCOR1, however, SCOR1 has a layer of sheet-type corrosion attached to it. SCOR2 is the thin sheet-type corrosion only. To ensure that the plates remain fixed in the center of the cylinders, they were attached to 250 mm long expanded metal cylinders, as shown in Figure 5 (a-b). The plates were attached to the expanded metal by using a polyurethane sealant. The specimen containing no metal plate also contained a cylinder of expanded metal, but no sealant. The concrete recipe was one part each of Portland cement and coarse aggregate, two parts fine aggregate, and enough water to achieve a water-to-cement ratio of 0.43. Details about the concrete recipe can be viewed in Table 1. PVC pipes were used as molds (see Figure 5 (c-d)) for the cylinders. The concrete cylinders were initially 250 mm long. After curing for 30 days, they were cut to lengths of 200 mm by removing 25 mm from each end. During casting the specimen containing SCOR2, it was observed that the thin corrosion product shattered. This caused multiple pieces of the corrosion product to be distributed across the entire volume.

Figure 4. Plate discs that were embedded in concrete. OK is a plate with no known flaws. COR is a uniformly corroded plate. SCOR1 is uniformly corroded and has a thin sheet corrosion product attached to it. SCOR2 consists only of the sheet-type corrosion product.

Figure 5. (a) Side-view of the expanded metal cylinder with the OK-plate attached to it. (b) Top-down view of the cylinder in (a). (c) Concrete cylinder immediately after casting. The total length of the concrete cylinder is here 250 mm, but the PVC pipe is longer. (d) Shows a concrete cylinder after being cut to length of 200 mm.

Table 1. Concrete recipe.

Concrete component	Mass [kg]
Portland cement	6.038
Coarse aggregate (4-8 mm)	6.038
Fine aggregate (0-2 mm)	12.08
Water	2.597

3.2.2 Experimental Setup for measuring Cross-Modulation

A schematic of the experimental setup used for the modulation experiments can be seen in Figure 6. The probe was a continuous sine wave with a frequency of 37 kHz and amplitude of 65 V_{pp}. The pump was an AM continuous sine with a carrier frequency of 178 kHz, modulation depth of 100%, and a modulation frequency of 100 Hz. With an AM excitation, it is the modulation component that activates the defects. The carrier frequency was chosen to be significantly higher than the probe-wave to separate any modulation between the pump carrier and the probe from the cross-modulation between the modulation component and the probe. The pump had a measured maximum amplitude of 130 V_{pp}. The equipment used is shown in Figure 6, except for the transducers. Tx1 and Rx were both Olympus X1021, and Tx2 was an Olympus X1019. Ultrasound gel was used as coupling between the transducers and the specimen. A script designed in LabView controls the instruments, collects data, and returns a power spectrum for each measurement. Additional post-processing was performed in MATLAB.

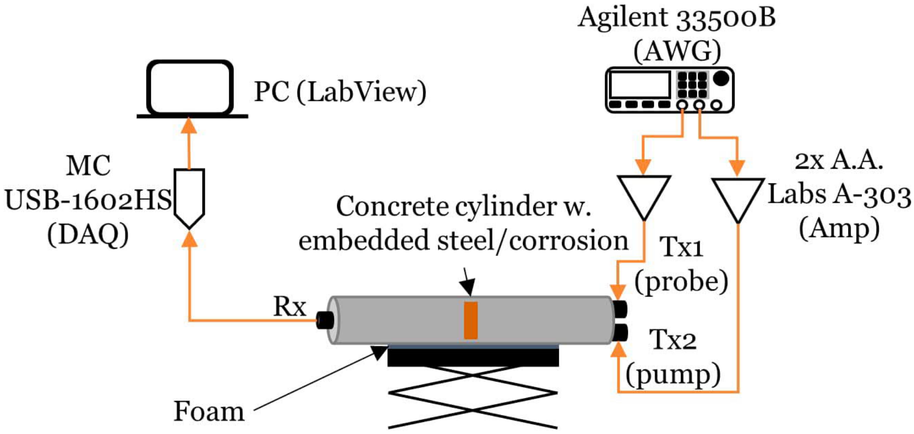

Figure 6. Schematic of the experimental setup used for the experiments on the concrete cylinders.

4. RESULTS AND DISCUSSIONS

4.1 Inspection of the Steel Plate using Second Harmonic Analysis

The magnitude spectra for the time signals recorded at points #4, #11, and #12 are plotted in Figure 7. Second harmonics (~9 MHz) are evidently generated at all measurement points. The magnitude of the second harmonic is greatest at point #4, which is located in the non-corroded region OK. Only studying harmonic amplitudes may yield erroneous conclusions as some inherent non-linearity is always to be expected. The important parameter is the energy distribution between linear and non-linear components, such as β' (Eq. 3). The β'-values averaged across all excitation levels obtained at the measurement points illustrated in Figure 2 are all plotted in Figure 8 to show the distribution across the plate. It is clear that no separation can be made between the OK and COR regions based on β'-values alone. However, there is a significant increase of β' in the SCOR region. Note that no attenuation correction has been applied.

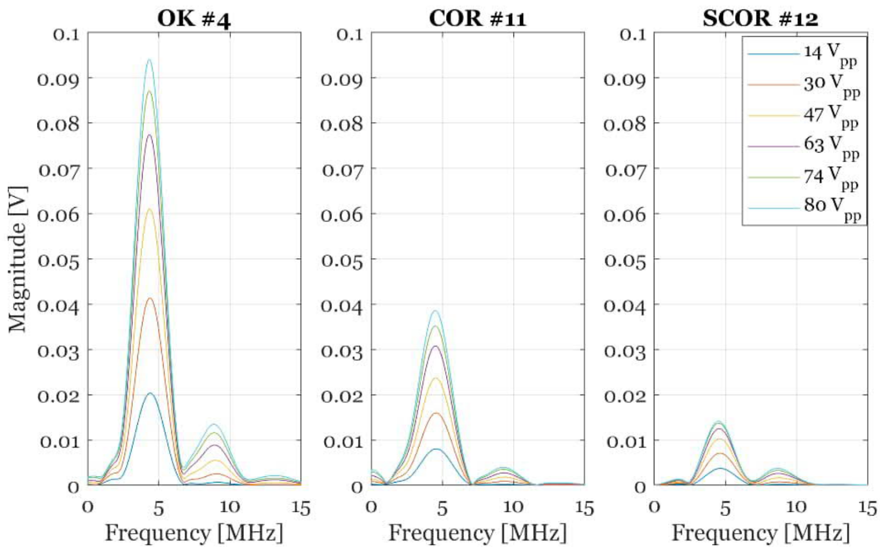

Figure 7. Magnitude spectra for the measurement points #4 (in OK region), #11 (COR region), and #12 (SCOR region). Figure reproduced from [5].

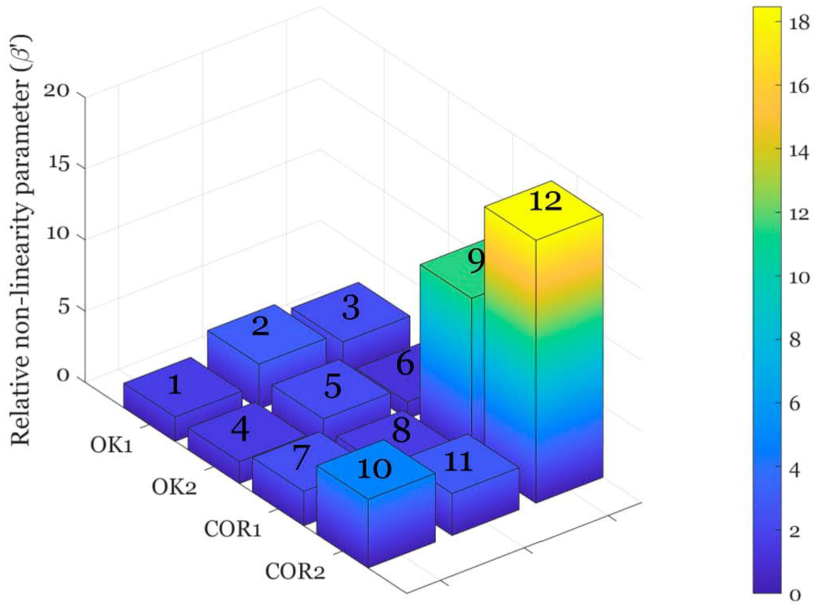

Figure 8. Averaged β'-values at all measurement points (indicated by Arabic numerals on the top surface of the bars). Figure reproduced from [5].

The interested reader is referred to Ref. [5] for additional in-depth analysis and discussion of this investigation.

4.2 Inspecting Concrete Cylinders with Cross-Modulation

The power spectra (PS) obtained from the measurements on the concrete cylinders can be viewed in Figure 9. The PS are plotted in dB-scale which makes it difficult to draw any conclusions by only studying the spectra as the magnitudes vary by several orders, but the information necessary for the determination of α (Eq. (4)) can be obtained. The sidebands appear to be ranging from 35 – 39 kHz. By integrating the linear scale PS in the regions 35 kHz – 36.94 kHz and 37.06 kHz– 39 kHz, the energy in the sidebands is obtained. The probe energy is computed by integrating the PS in the interval 36.94 kHz – 37.06 kHz. The corresponding α for each specimen can be viewed in Figure 10. It is shown that the level of non-linearity is highest for the specimen containing uniform and shell corrosion (SCOR1). SCOR2 and the specimen without embedded steel have almost equal α. The shattering of the sheet corrosion during casting likely affected the probability of detection as small pieces of the corrosion product were distributed in the entire volume. Future experiments with higher probe-wave frequency aim to investigate the feasibility of detecting this distributed 'damage' as a higher-frequency probe wave will scatter when interacting with aggregates, and possibly small corrosion products. The high level of non-linearity seen at OK could possibly be explained by the concrete not properly binding to the plate surface, as it is very smooth in comparison to the other plates. Any delamination would cause an increase in non-linearity. However, as these results are based on single measurements the variation in parameter values is unknown. Observe that no attenuation correction has been made which also affect the results. Continued work will focus on designing repeatable measurements of non-classical non-linearity on concrete samples containing embedded corrosion by investigating the impact of the experimental conditions. Investigations of the impact of couplant between sensors and the sample, the contact pressure applied to the sensors, and more will be conducted.

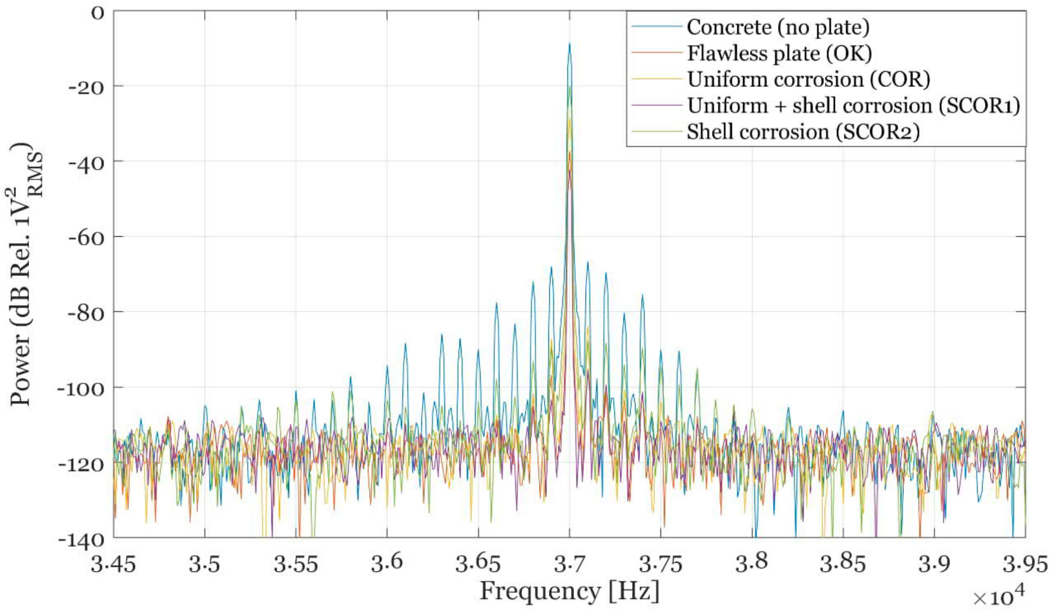

Figure 9. Power spectra for all concrete specimens.

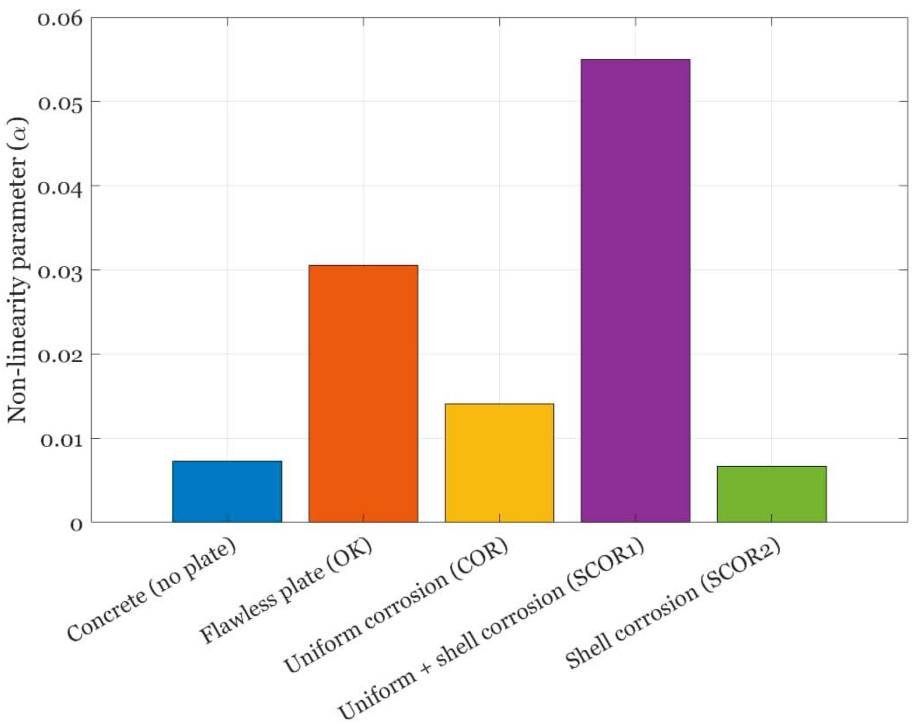

Figure 10. The non-linearity parameter α for the inspected specimens.

5. CONCLUSIONS

The current studies into the feasibility of using non-linear ultrasound to detect embedded corrosion indicate some potential of the methods. Second harmonic analysis accurately indicated the area with the most severe type of corrosion, the shell type. This corrosion product is characterized by the presence of gross damage. Initial testing on concrete specimens with embedded steel plates using the cross-modulation technique indicates further potential of non-linear ultrasonics. Due to the complexity of non-linear mechanisms, it is generally difficult to determine the exact sources of non-linearity. However, by utilizing phenomena that arise due to non-classical non-linearity, such as the cross-modulation treated in the present work, masking effects from inherent classical non-linearities might be reduced.

ACKNOWLEDGEMENTS

This work is supported by funding from The Swedish Energy Research Centre (Energiforsk BET165) and the Swedish Radiation Safety Authority (SSM2019-1114). Gratitude is addressed towards Johanna Spåls (Ringhals AB) for granting us access to the Ringhals 3 corrosion product.

REFERENCES

[1] V. Y. Zaitsev, L. A. Matveev, and A. L. Matveyev, "On the ultimate sensitivity of nonlinear-modulation method of crack detection," *NDT E Int.*, vol. 42, no. 7, pp. 622–629, 2009, doi: 10.1016/j.ndteint.2009.05.001.

[2] C. M. Hedberg, E. Johnson, S. A. K. Andersson, K. C. E. Haller, G. Kjell, and S. E. Hellbratt, "Ultrasonic monitoring of a fiber reinforced plastic - Steel composite beam during fatigue," *Proc. 6th Eur. Work. - Struct. Heal. Monit. 2012, EWSHM 2012*, vol. 2, pp. 1254–1260, 2012.

[3] Kyung-Young Jhang, C. J. Lissenden, I. Solodov, Y. Ohara, and V. Gusev, *Measurement of Nonlinear Ultrasonic Characteristics*. Singapore: Singapore Nature Singapore Pte Ltd, 2020.

[4] T. Kundu, Ed., *Nonlinear ultrasonic and Vibro-acoustical techniques for Nondestructive evaluation*. Springer Nature Switzerland AG, 2018.

[5] M. Nilsson, P. Ulriksen, and N. Rydén, "Nonlinear ultrasonic characteristics of a corroded steel plate," *Nondestruct. Test. Eval.*, vol. 00, no. 00, pp. 1–24, 2022, doi: 10.1080/10589759.2022.2123481.

[6] B. D. H. Tellegen, "Interaction Between Radio-Waves?," *Nature*, vol. 131, p. 840, 1933.

[7] V. Zaitsev, V. Gusev, and B. Castagnede, "Luxemburg-Gorky Effect Retooled for Elastic Waves: A Mechanism and Experimental Evidence," *Phys. Rev. Lett.*, vol. 89, no. 10, pp. 2–5, 2002, doi: 10.1103/PhysRevLett.89.105502.

[8] V. Y. Zaitsev, V. Gusev, and B. Castagnède, "Observation of the 'Luxemburg-Gorky effect' for elastic waves," *Ultrasonics*, vol. 40, pp. 627–631, 2002.